수의학석사 학위논문

Anatomic Evaluation of Normal Laryngeal Region Using Magnetic Resonance Imaging under Intravenous Anesthesia in Dogs

개에서 정맥마취 하 자기공명영상을 통한 정상 후두 부위의 해부학적 평가

2023년 02월

서울대학교 대학원

수의학과 임상수의학 전공

백 록 담

Anatomic Evaluation of Normal Laryngeal Region Using Magnetic Resonance Imaging under Intravenous Anesthesia in Dogs

지도교수 최 지 혜

이 논문을 수의학석사 학위논문으로 제출함

2022년 10월

서울대학교 대학원
수의학과 임상수의학 전공
백 록 담

백록담의 수의학석사 학위논문을 인준함

2023년 01월

위 원 장 _____ (인)

부위원장 _____ (인)

위 원 _____ (인)

Abstract

Anatomic Evaluation of Normal Laryngeal Region Using Magnetic Resonance Imaging under Intravenous Anesthesia in Dogs

Loktam Baek
Major in Veterinary Clinical Sciences
Department of Veterinary Medicine
The Graduate School
Seoul National University

In veterinary medicine, magnetic resonance (MR) imaging to the laryngeal region requires anesthesia because of its long image acquisition time. Tracheal intubation for respiratory anesthesia can displace the laryngeal structures and obscure or distort the pathologic lesion of this area. The purpose of this study was to assess the clinical applicability of MR imaging to the laryngeal region in dogs under intravenous anesthesia without tracheal intubation. In this prospective, method comparison study, MR and CT images of the laryngeal regions were acquired using

1.5-Tesla MR scanner and 64-slice CT scanners in five clinically healthy, purpose-bred male beagle dogs under general anesthesia without intubation respectively. Then, MR images were compared with the pre- and post-contrast CT images and assessed the conspicuity of the laryngeal structures and discrimination of some structures, and comparative evaluation of the clinical feasibility of both imaging techniques was conducted.

MR scan of the laryngeal region was successfully completed in all dogs under intravenous anesthesia without tracheal intubation. On the MRI rather than CT, the conspicuity of the vocal ligament and laryngeal muscle, differentiating the internal components of the thyroid cartilage, cricoid cartilage, epiglottis, and distinguishing vessel wall from the lumen were considered more appropriate to evaluate. On the other hand, CT was more useful than MRI for identifying the cricoid cartilage, thyroid cartilage, and hyoid bone. On the MR images, Artifacts thought to be caused by movement during respiration were confirmed to a minor extent that obscured the boundary between the arytenoid cartilage and the air-filled cavity, and did not interfere with the image evaluation. MRI is feasible modalities for the evaluation of the laryngeal region. The three observers had excellent agreement across all evaluation categories statistically.

Furthermore, according to the detailed structures, each modality had a different range of applicability. Depending on where the lesion is suspected to be, the study's findings may be used as a guideline for selecting an imaging modality.

Keywords: computed tomography, dog, laryngeal region, magnetic resonance imaging

Student Number: 2021-26846

Table of Contents

Introduction 1

Materials and Methods 4

1. Selection and description of subjects 4
2. Anesthesia and schedule 5
3. CT examination 6
4. MR imaging 7
5. Image analysis 8
6. Statistical analysis 11

Results 12

1. CT and MR images acquisition of the laryngeal region 12
2. CT images of the laryngeal region 13
3. MR images of the laryngeal region 17
4. Comparison between CT and MR images 21

Discussion 37

References 42

국문초록 46

Introduction

The larynx is a musculocartilaginous part of the upper respiratory system located just before the tracheal entrance and plays a major role in breathing by controlling the airflow and providing the air passage, swallowing, and vocalization (Evans et al., 2012). Several diseases can affect the larynx in dogs including laryngeal paralysis, laryngeal collapse, and laryngeal mass (MacPhail, 2020). In particular, laryngeal tumors or pathologic legions from the surrounding structures which can distort, displace, or obstruct the larynx can cause coughing or gagging when eating or drinking, noisy panting, increased panting, respiratory distress, and difficulty in swallowing. Although laryngeal tumors is not commonly identified in dogs, various primary laryngeal tumors such as adenoma, adenocarcinoma, papilloma, squamous cell carcinoma, chondroma, chondrosarcoma, fibroma, fibrosarcoma, rhabdomyoma, and rhabdomyosarcoma has been reported in dogs (Carlisle et al., 1991).

The diagnosis of the laryngeal disease is made mainly through laryngoscope and biopsy (Teixeira et al., 2014). In addition, diagnostic imaging such as computed tomography (CT) and magnetic resonance (MR) imaging plays an important role to delineate the laryngeal lesions in human because the larynx is an anatomically complex structure including epiglottis, vestibule, thyroid cartilage, and others which are made of the cartilage, ligaments, and muscles. CT and MRI can evaluate the structures and spaces in deep location, and the extent of the lesion without superimposition, and plays an essential and complementary role in staging

of the laryngeal tumor and making a plan and post-operative evaluation (Wu et al., 2016). In addition, it can be used to diagnose non-neoplastic diseases such as laryngoceles, trauma, paralysis, and inflammation of the larynx (Becker et al., 2008).

Similarly, in veterinary medicine, when the laryngeal diseases are suspected, radiography is used for screening the cervical region because it is fast and easily accessible. However, radiographic evaluation of the laryngeal lesion is limited due to the nature complexity of the laryngeal region showing similar radiographic density within small area (Carlisle et al., 1991). CT has been applied to assess the laryngeal region in normal dog and dogs with upper airway obstruction or laryngeal tumor cases (Dunbar et al., 2012; Stadler et al., 2011). CT scans require a short time and CT images can be obtained in respiratory compromised dogs only under sedation or even awake condition.

Meanwhile, MR features of the laryngeal structure was described in one study by cross-sectional comparison with the actual cadaver in the normal dogs (Vázquez et al., 1998). Unlike human, clinical application of MR imaging to the laryngeal lesion is limited in dogs, although superior soft tissue resolution can be expected in MR images compared to CT images. This result would be related with the need of anesthesia and long images acquisition time. Moreover, the tracheal tube can displace the normal laryngeal structures and make the images evaluation difficult, although it secures the airway.

Recently, as technology advances in MR imaging, it does not require very deep anesthesia and faster scanning acquisition can be performed (Elders et al., 2019). Therefore, in this study, MR imaging of the laryngeal region were

conducted in healthy dogs after intravenous anesthesia without tracheal intubation and compared with CT images as reference. The purpose of this study was to assess the feasibility of MR imaging for laryngeal evaluation in dogs under intravenous anesthesia, (2) to describe the MR features of the laryngeal structures compared in CT, and (3) to present the MRI indication for delineating the laryngeal structures in dogs. It was hypothesized that MR imaging of the laryngeal region would be possible with only intravenous anesthesia without tracheal intubation and MR images would be superior to delineate the soft tissue structures than CT.

Materials and Methods

1. Selection and description of subjects

This prospective, method comparison study was performed in 5 purpose-bred male beagle dogs. The mean age of the dogs was 4.4 years (range, 4 – 6 years), and the mean body weight was 14.4 kg (range, 12.8 – 15.5 kg). The dogs were individually housed and fed commercial dry food and tap water *ad libitum*. None of the dogs had histories or clinical signs indicative of respiratory diseases. All dogs were clinically healthy based on physical examination, auscultation, complete blood count, serum biochemistry, and cervical and thoracic radiography. Radiographs were acquired with a digital radiographic system (EVA-HF525, Gemss-Medical, South Korea) using maximum tube voltage 125 kV and maximum tube current 500 mA with a cesium-iodine based flat panel detector (FDX4343R, Gemss-Medical) integrated into the table. The right lateral and ventrodorsal views of cervical and thoracic radiographs were taken and then all radiographs were assessed on picture archiving and communications systems (Infinitt PACS, Infinitt Healthcare, Seoul, Korea) by two veterinarians (S.A., S.L.) with one-years of radiology experience. All procedures were conducted under the approval of Seoul National University institution's animal care and use committee (SNU-220810-2).

2. Anesthesia and schedule

After fasting at least for 12 hours, a 24-gauge catheter was placed into the cephalic vein for the anesthesia. Acepromazine (0.01 mg/kg, Sedaject®, SamuMedian Co., South Korea) and medetomidine (0.01 mg/kg, Domitor®, Zoetis, Finland) were administered intravenously for each CT and MR examination. The anesthesia was maintained without intubation in all dogs. During MR scan, the dog's condition was monitored through real-time camera images, and additional anesthesia (medetomidine, 0.01 mg/kg) was injected when the dog showed slight movement. Additional anesthetic was given approximately 30-minute intervals. In each dog, CT and MRI scans were performed within one day. CT scans were performed first, then it took about 15 minutes to move and prepare the dog for the subsequent MRI scan.

After CT and MRI, the general condition and side effects related to anesthesia or contrast medium, such as respiratory signs, vomiting, depression, and anorexia, were monitored in each dog for 3 days.

3. CT examination

Immediately after anesthesia, each dog was positioned in sternal recumbency, with the head in the isocenter of the gantry. CT images of the laryngeal region were obtained using the 64-slice CT scanner (Aquillion 64™, Toshiba Medical Systems, Tochigi, Japan). The scan range covered from the root of tongue to the level of 3rd tracheal ring. CT images were obtained in each dog 120 kVp, 200 mAs, 512 x 512 matrix, slice thickness 1.0 mm, and pitch factor 0.828. After pre-contrast CT scanning, the post-contrast CT scan was performed after manual injection of 2 ml/kg iohexol (OMNIPAQUE™, GE Healthcare Co., Ltd, China). During CT scanning, the dog was allowed to breathe freely without inducing apnea.

All acquired CT images were reconstructed with 1 mm slice thickness, 1 mm intervals into the transverse, sagittal, and dorsal planes. Reconstructed images were evaluated using soft tissue window with window level of 30 Hounsfield Unit (HU) and window width of 320 HU, and using bone window with window level of 450 HU and window width of 1500 HU.

4. MR imaging

MR imaging was performed after placing the dog in sternal recumbency, using a 1.5T-MRI scanner (GE Signa 1.5T, GE healthcare, Illinois, US) with an 8-channel knee coil. The range of scan was same as that of CT scanning. In each dog, T2-weighted (T2W, TR = 5000 ms, TE = 80 ms, slice thickness = 3 mm), T1-weignted (T1W, TR = 450 ms, TE = 9 ms, slice thickness = 3 mm) and T1W-contrast enhanced images (T1W-CE) after intravenous injection of 0.2 ml/kg gadolinium-based contrast agent (Dotarem, Guerbet, Villepinte, France) were acquired in the transverse, sagittal and dorsal planes.

5. Image analysis

All obtained MR and CT images were evaluated on PACS System (INFINITT PACS, Infinitt Healthcare, Seoul, South Korea) and compared each other at the same cross-sectional levels (**Fig 1**). Nine transverse images obtained at 3 mm intervals from the middle level of the epiglottis and additional one image obtained at the first tracheal cartilage level were used for analysis. Image evaluation was performed independently by three observers; one veterinarian (L.B.) with two years radiology experiences, and two veterinarians (S.A., S.L.) each with one-year radiology experience blinded to the other's results.

MR images of the laryngeal regions were assessed about the conspicuity of the larynx and surrounding structures, inner discrimination of the internal components of some structures, and compared with the CT images of each structure. The conspicuity of the laryngeal and surrounding structures was evaluated from the arytenoid cartilage, cricoid cartilage, thyroid cartilage, vestibular fold, vocal ligament, laryngeal muscle, hyoid apparatus, mandibular and retropharyngeal lymph nodes, mandibular salivary glands, thyroid glands, and large vessels such as carotid artery and vein. The conspicuity of the larynx and surrounding structures were assessed based on the degree of the recognition of the structure from others and scored on a 3-point scale: 1 = insufficient, when the structure's identification is limited, 2 = adequate, when the structure can be easily recognized, and 3 = optimal, when the structure can be easily recognized with clear margin. In addition, discrimination of the internal components were evaluated from the epiglottis, cricoid cartilage thyroid cartilage and vessels based on the

distinctions between the internal components of the structure that are visually distinct, and scored on a 3-point scale: 1 = insufficient, 2 = adequate, when there is a lesion in the corresponding structure, and 3 = optimal, when the texture difference from the nearby structure can be clearly noticed.

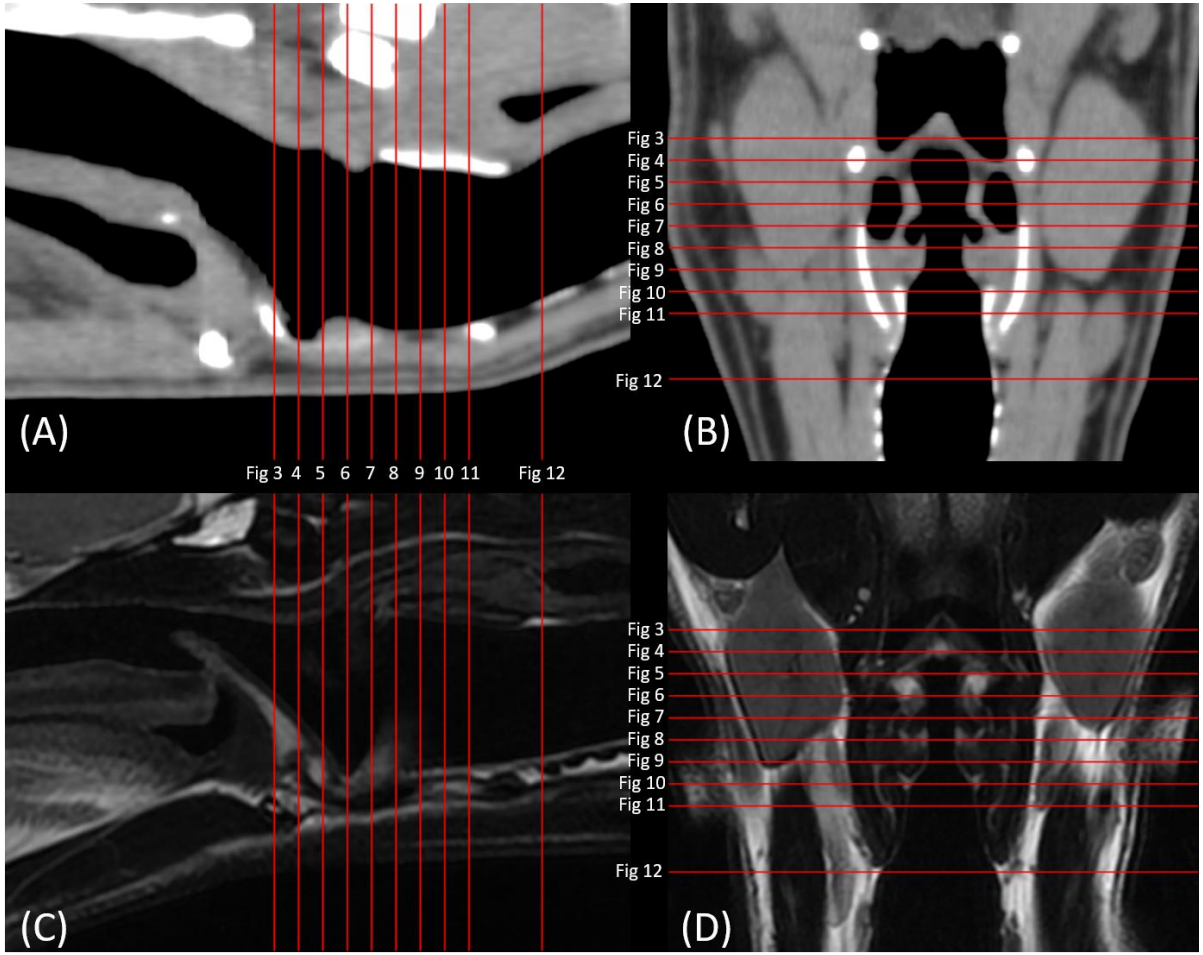

FIGURE 1. Midsagittal pre-contrast CT (A), T2W MRI (C), and dorsal pre-contrast CT (B), T2W MRI (D) of laryngeal region. The 10 lines in each image, from cranial to caudal direction, denote the schematic locations of the transverse sections that correspond to figure 3 through figure 12. The right side of the image in dorsal plane is the left side of the animal.

6. Statistical analysis

Statistical analysis was performed by one observer (L.B.), under the supervision of one statistician (J.R.P.), using IBM SPSS 26.0 software (IBM Corporation, NY). The interclass correlation coefficient test was used to analyze the agreement between three observers for each evaluation criteria. Interobserver agreements were analyzed using the intraclass correlation coefficient (ICC) test: ICC < 0.4, poor agreement; ICC 0.41–0.6, moderate agreement; ICC 0.61–0.8, good agreement; ICC > 0.8, excellent agreement (Perinetti, 2018). The differences in the degree of conspicuity of the structure and the degree of discrimination of the internal components of some structures between CT and MRI, and between MRI sequences were analyzed using Wilcoxon signed ranks test. All data were presented as mean ± standard deviation. P values of less than 0.05 were considered significant.

Results

1. CT and MR images acquisition of the laryngeal region

CT and MR images of the laryngeal region was obtained successfully in all dogs using intravenous anesthesia without tracheal intubation. The pre- and post-contrast CT images were obtained within 10 minutes in a neutral, sternal recumbent position, without additional anesthesia in all dogs. Meanwhile, the average scan time of total MR sequences was about 60 min in each dog. Additional anesthesia during total procedure using medetomidine (0.01 mg/kg) was performed two or three times in each dog.

2. CT images of the laryngeal region

The qualitative assessments of the laryngeal regions on the pre- and post-contrast CT images are presented in **Table 1** and **Table 2**. **Table 1** compares the conspicuity of the laryngeal structures, and **Table 2** compares the degree of differentiation between the internal components of some structures. Most laryngeal structures were visualized similarly on pre- and post-contrast CT images without significant difference in conspicuity or internal components discrimination of the laryngeal structures, only except for the vessels, enhanced brightly after contrast injection (**Fig 8**). The large blood vessels could be defined the vascular margin and localized on both pre- and post-contrast CT images. However, smaller vessels were distinguishable from the adjacent structures which showed similar density only after contrast injection. Both pre- and post-contrast images, the vessel wall and lumen were not distinguished. The soft palate and laryngeal muscles showed homogeneous soft tissue density similarly regardless of the contrast injection. The post-contrast CT images were not helpful for improving the conspicuity of the muscles unless their margins were spatially separated.

The epiglottis was shown as a concave shaped structure with an epiglottic cartilage as a framework and is surrounded by an epithelial layer (**Fig 3**). Except for cases where the cartilage was calcified, CT images did not clearly distinguish the inner cartilage from the outer epithelial layer. The arytenoid cartilage appeared as soft tissue density, except for the focal hyperdense area due to calcification (**Fig 4-7**). The thyroid and cricoid cartilages showed high attenuation and they were clearly differentiated each other (**Fig 8-11**). The thyroid cartilage surrounded the

ventral border of the larynx as a U-shaped. The cricoid cartilage was visualized as an annular ring structure with a wider dorsal part than ventral part and was distinct hyperdense.

The hyoid bone appeared distinct hyperdense on CT images and the shape of the hyoid apparatus was clearly visualized on volume rendering images (**Fig 3, 13**).

The air-filled structures, such as the laryngeal cavity, piriform recess, epiglottic vallecula, laryngeal vestibule, and tracheal lumen, were hypoattenuating, and the borders of the piriform recess and laryngeal ventricle were clear.

The inside of the tongue was distinguished with relatively low density, and the margins and septum with high density. The blood vessel distribution in the tongue was clearly observed after contrast injection.

TABLE 1. Conspicuity of the laryngeal structures on pre- and post-contrast CT images in healthy dogs

Evaluation structures	Scores		P-value
	Pre	Post	Pre : Post
Arytenoid cartilage, Cuneiform process	1.40±.55	1.40±.55	1.00
Arytenoid cartilage, Corniculate process	2.40±.55	2.40±.55	1.00
Cricoid cartilage	3.00±.00	3.00±.00	1.00
Thyroid cartilage	3.00±.00	3.00±.00	1.00
Vestibular fold	2.00±.00	1.80±.45	.32
Vocal ligament	1.00±.00	1.00±.00	1.00
Laryngeal muscle	1.00±.00	1.00±.00	1.00
Hyoid apparatus	3.00±.00	3.00±.00	1.00
Lymph nodes (mandibular, retropharyngeal)	3.00±.00	3.00±.00	1.00
Salivary glands (mandibular)	3.00±.00	3.00±.00	1.00
Thyroid glands	2.80±.45	3.00±.00	.32
Vessels	3.00±.00	3.00±.00	1.00

Score data is presented as mean ± SD score

*Within a row, corresponding structures with superscripted letters differ significantly between the MRI sequences ($P < .05$)

Pre, pre-contrast CT images; Post, post-contrast CT images

TABLE 2. Discrimination of the internal components of the laryngeal structures on pre- and post-contrast CT images in healthy dogs

Evaluation structures	Plane	Scores		P-value
		Pre	Post	Pre : Post
Epiglottis	Transverse	1.00±.00	1.20±.45	.32
Epiglottis	Sagittal	1.40±.55	1.40±.55	1.00
Cricoid cartilage	Transverse	1.00±.00	1.00±.00	1.00
Thyroid cartilage	Transverse	1.00±.00	1.00±.00	1.00
Vessels	Transverse	1.00±.00	1.00±.00	1.00

The degree of discrimination was scored as: optimal (3 points); adequate (2 points); insufficient (1 point).

Score data is presented as mean ± SD score

*Within a row, corresponding structures with superscripted letters differ significantly between the MRI sequences ($P < .05$)

Abbreviations: Pre, pre-contrast CT images; Post, post-contrast CT image

3. MR images of the laryngeal region

In the laryngeal regions, all evaluation structures were observed on transverse plane of all MR images regardless of MR sequences or contrast study. **Table 3** compares the conspicuity of laryngeal structures, and **Table 4** compares the degree of internal component differentiation in specific structures by MR sequences.

On the sagittal section of the epiglottis, the inner cartilage was clearly distinguished with a high signal intensity and the outer epithelial layer with a relatively low signal intensity in all T2W, T1W, and T1W-CE images (**Fig 2**). In transverse images, the distinction between the components was less clear than in sagittal images (**Fig 3**).

The thyroid, cricoid, and arytenoid cartilages were observed individually in the MRI image. In the arytenoid cartilage, the anterior corniculate process was accompanied by a significant amount of artifact, so the boundary was unclear, and the posterior part was relatively clearly imaged (**Fig 4-7**). The thyroid cartilage visualized a clear low signal compared to surrounding muscles in the T2W images and a relatively high signal intensity in the T1W images (**Fig 6-9**). The cricoid cartilage was a low signal intensity in T2W and isointense to adjacent muscles in T1W (**Fig 9-11**).

The air-filled cavities and lumen showed distinct signal void. Compared to CT image, the borders of piriform recess and laryngeal ventricle were slightly blurred on MRI.

The vocal ligament formed the anterior boundary of the vocal fold, and was identified as a pair of linear structures from the vocal process of the arytenoid

cartilage to the dorsal side of the thyroid cartilage. On CT image, vocal ligament was indistinguishable, however, on MRI, it was identified as a hyperintense, linear structure (**Fig 7**).

The contrast between the laryngeal muscles was more pronounced in the T2W image than in the T1W image. Muscles appear as relative isointense to adjacent cartilages on T1W images in general, and despite the image's homogeneity, it is still feasible to determine the boundaries of the muscles to some extent (**Fig 7-10**).

In contrast to CT, the hyoid bones showed iso- to low signal intensity on MR image, and the contrast with the surrounding structures was less pronounced (**Fig 3**). The cross section of blood vessel was clearly identified, and it was possible to distinguish the vessel wall from the lumen in both the T1W and T2W images (**Fig 12**).

In the MR image, it was possible to confirm even more detailed structures of the tongue than in the CT scan. The tongue showed hyperintense compared to the surrounding muscles on T1W and T2W images, furthermore, on the sagittal plane, it was possible to confirm even the texture and boundaries of the tongue muscles. Compared with CT image, the border of the soft palate was more clearly seen in MRI, and the detailed signal differences in the parenchyma was observed, which was more clearly identified on the T2W image (**Fig 2**).

Overall conspicuity of the laryngeal muscle showed a significantly higher score in the T2W than in the T1W (**Table 3**). No significant difference was found when comparing T1W and T1W-CE images (**Table 3, 4**).

TABLE 3. Conspicuity of the laryngeal structures on the transverse planes of MR images obtained using T1 and T2-weighted sequences in healthy dogs

Evaluation structures	Scores			P-Value	
	T2W	T1W	T1W-CE	T1W vs. T2W	T1W vs.T1W-CE
Arytenoid cartilage, Cuneiform process	2.20±.45	2.00±.00	1.60±.89	.32	.32
Arytenoid cartilage, Corniculate process	2.80±.45	2.40±.55	2.40±.55	.32	1.00
Cricoid cartilage	2.20±.45	1.80±.45	1.60±.55	.16	.32
Thyroid cartilage	2.60±.55	2.00±.00	1.80±.45	.08	.32
Vestibular fold	2.60±.55	2.40±.55	2.80±.45	.32	.16
Vocal ligament	2.75±.50	2.50±.58	2.75±.50	.16	.16
Laryngeal muscle	3.00±.00	1.80±.45	2.00±.00	.03*	.32
Hyoid apparatus	2.60±.55	2.00±.00	2.20±.45	.08	.32
Lymph nodes (mandibular, retropharyngeal)	3.00±.00	3.00±.00	3.00±.00	1.00	1.00
Salivary glands (mandibular)	3.00±.00	3.00±.00	3.00±.00	1.00	1.00
Thyroid glands	3.00±.00	3.00±.00	3.00±.00	1.00	1.00
Vessels	3.00±.00	3.00±.00	3.00±.00	1.00	1.00

* $P < 0.05$, Data is presented as mean ± standard deviation.

T2W, T2-weighted; T1W, T1-weighted; T1W-CE, contrast-enhanced T1-weighted.

TABLE 4. Discrimination of the internal components of the laryngeal structures on MR images obtained using T1 and T2-weighted sequences in healthy dogs

Evaluation structures	Plane	Scores			P-Value	
		T2W	T1W	T1W-CE	T1W:T2W	T1W:T1W-CE
Epiglottis	Transverse	2.20±.45	2.20±.45	2.20±.45	1.00	1.00
Epiglottis	Sagittal	2.80±.45	2.80±.45	2.80±.45	1.00	1.00
Cricoid cartilage	Transverse	2.00±.71	1.80±.45	2.00±.71	.32	.56
Thyroid cartilage	Transverse	1.20±.45	1.80±.45	2.20±.45	.08	.16
Vessels	Transverse	3.00±.00	2.60±.55	3.00±.00	.16	.16

* $P < 0.05$

Data is presented as mean ± standard deviation.

T2W, T2-weighted; T1W, T1-weighted; T1W-CE, contrast-enhanced T1-weighted.

4. Comparison between CT and MR images

Based on the 95% confident interval of the intraclass correlation coefficient estimate, values were 0.998 for CT scores, 0.973 for MRI scores, indicative of both excellent reliabilities. Statistical processing of comparative evaluation for each structure was performed based on data of (L.B).

Table 5 presents the comparative evaluation of the degree of conspicuity of each structure constituting the larynx shown on pre- and post-contrast CT images, and T1W, T2W, and T1W-CE of MR images. The distinction between the inner cartilage and the surrounding membrane layer for the thyroid, cricoid, and epiglottis, as well as the distinction between the wall and the lumen for vessels are presented in **Table 6**. MRI scores were significantly higher than CT scores for identifying the overall laryngeal muscle and vocal ligament. In contrast, the scores for discrimination of the hyoid apparatus were significantly higher in CT than in MRI. MR images showed significantly higher scores than CT images for distinguishing the inner cartilage and outer epithelial, and connective tissue layers of the epiglottis. Also, while MRI scores were significantly higher for differentiating between the inner cartilage and its surrounding perichondrium in thyroid and cricoid cartilage, CT scores were significantly higher for identifying the structures. In distinction between vessel lumen and wall, MRI showed significantly higher scores than CT.

From **Figure 3 to Figure 12**, the transverse images of the level indicated in **Figure 1** were sequentially arranged from cranial to caudal direction, and T1W, T2W MRI, pre-, and post-contrast CT images of the same cross section were

presented in each figure. **Figure 13** presents the 3D volume rendering image of laryngeal region.

TABLE 5. Comparison between CT and MRI for conspicuity of the laryngeal structures on the transverse planes in five dogs

Evaluation structures	Scores		P-value
	MRI	CT	MRI : CT
Arytenoid cartilage, Cuneiform process	1.93±.43	1.40±.55	.48
Arytenoid cartilage, Corniculate process	2.53±.18	2.40±.55	.22
Cricoid cartilage	1.87±.38	3.00±.00	.04*
Thyroid cartilage	2.13±.30	3.00±.00	.04*
Vestibular fold	2.60±.43	1.90±.22	.07
Vocal ligament	2.67±.41	1.00±.00	.04*
Laryngeal muscle	2.26±.15	1.00±.00	.03*
Hyoid apparatus	2.27±.28	3.00±.00	.04*
Lymph nodes (mandibular, retropharyngeal)	3.00±.00	3.00±.00	1.00
Salivary glands (mandibular)	3.00±.00	3.00±.00	1.00
Thyroid glands	3.00±.00	2.90±.22	.32
Vessels	3.00±.00	3.00±.00	1.00

*P < 0.05

Data is presented as mean ± standard deviation.

TABLE 6. Comparison between CT and MRI for discrimination of the internal components of the laryngeal structures in five dogs

Evaluation structures	Plane	Scores		P-Value
		MRI	CT	MRI : CT
Epiglottis	Transverse	2.20±.30	1.10±.22	.04*
Epiglottis	Sagittal	2.80±.45	1.40±.54	.04*
Cricoid cartilage	Transverse	1.93±.49	1.00±.00	.04*
Thyroid cartilage	Transverse	1.73±.37	1.00±.00	.04*
Vessels	Transverse	2.87±.18	1.00±.00	.04*

*P < 0.05

Data is presented as mean ± standard deviation.

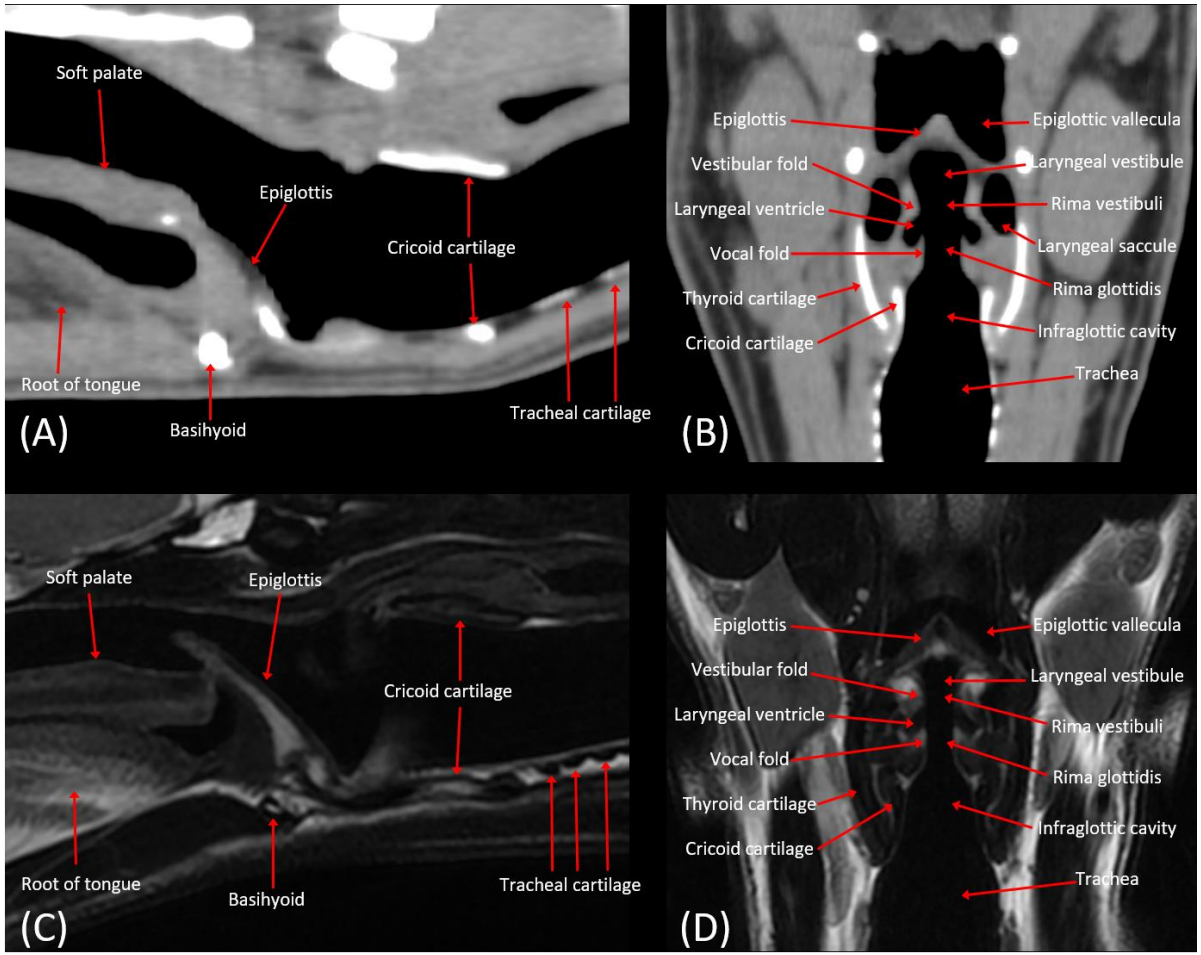

FIGURE 2. The images are the same as in figure 1 (A-D). The structure that each arrow points to is indicated by its name

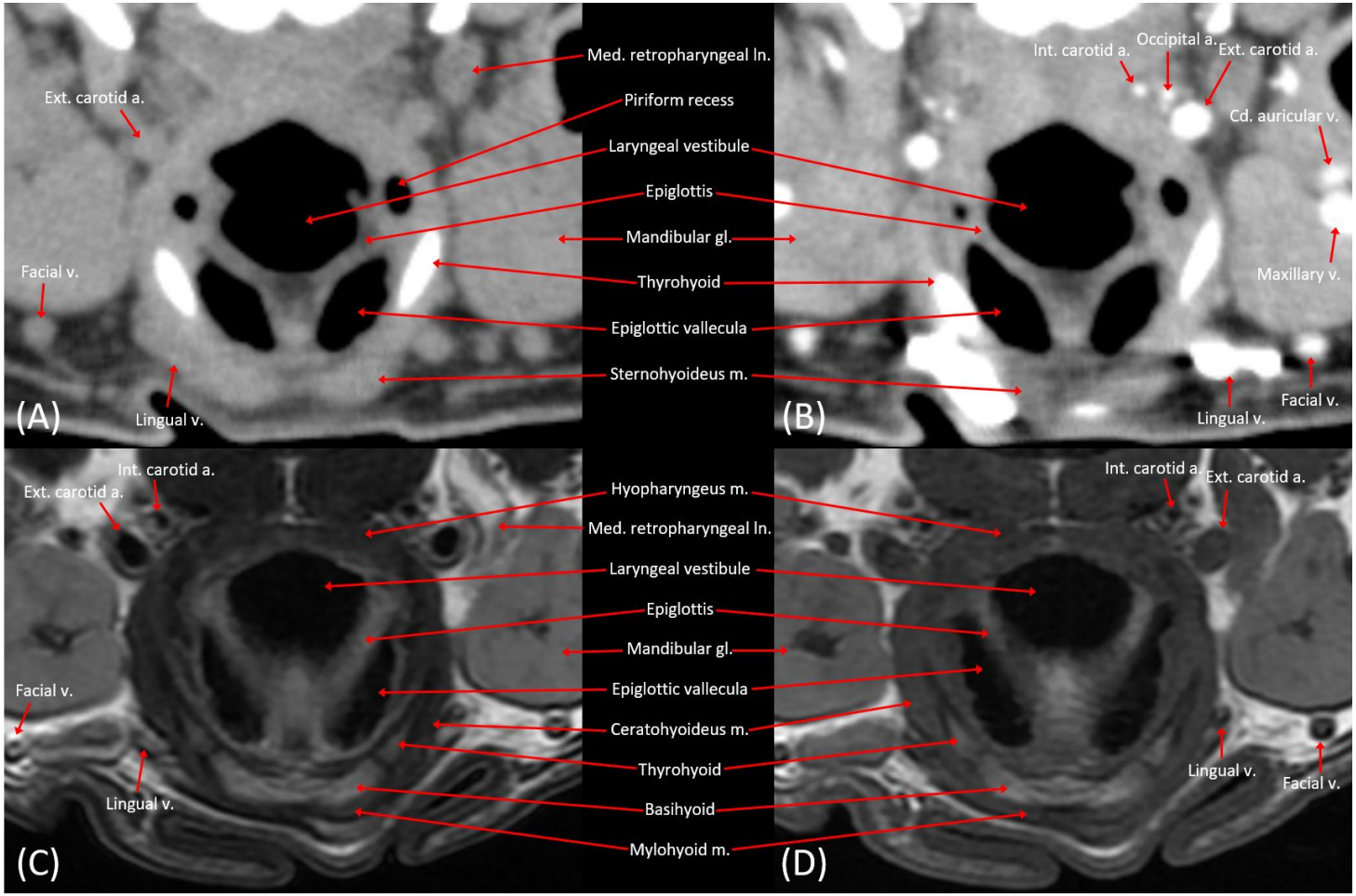

FIGURE 3. Transverse pre- (A) and post-contrast CT (B) images, T2-weighted (C) and T1-weighted MRI (D) at the epiglottic base level (CT window level: 30 HU, window width: 320 HU). The structure that each arrow points to is indicated by its name. The right side of each image is the left side of the animal. Abbreviations: a., artery; Cd. caudal; Ext., external; gl., gland; Int., internal; ln., lymph node; Med., medial; m., muscle; v., vein.

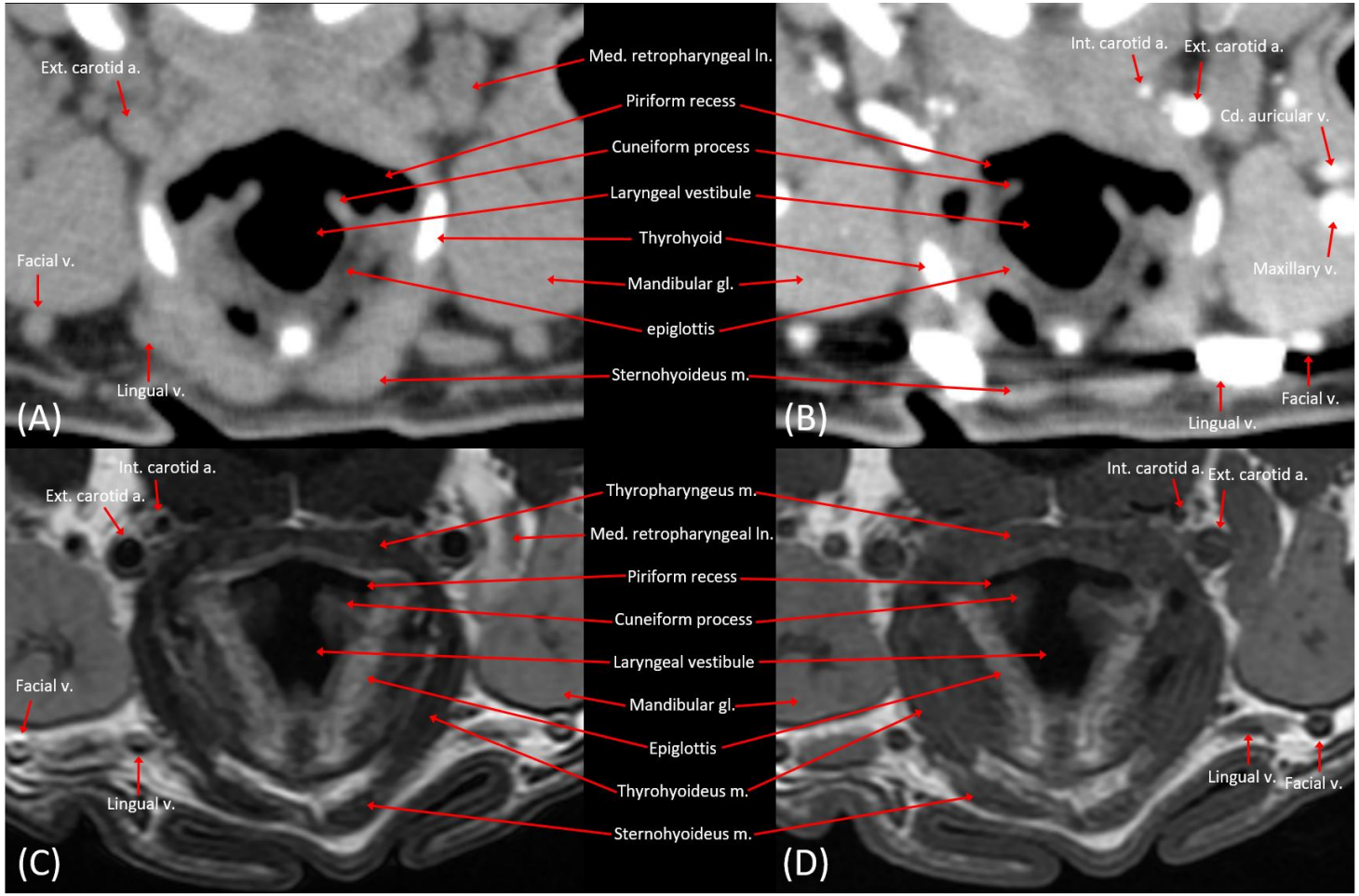

FIGURE 4. Transverse pre- (A) and post-contrast CT (B) images, T2-weighted (C) and T1-weighted MRI (D) at the cuneiform process level (CT window level: 30 HU, window width: 320 HU). The structure that each arrow points to is indicated by its name. The right side of each image is the left side of the animal. Abbreviations: a., artery; Cd. caudal; Ext., external; gl., gland; Int., internal; ln., lymph node; Med., medial; m., muscle; v., vein.

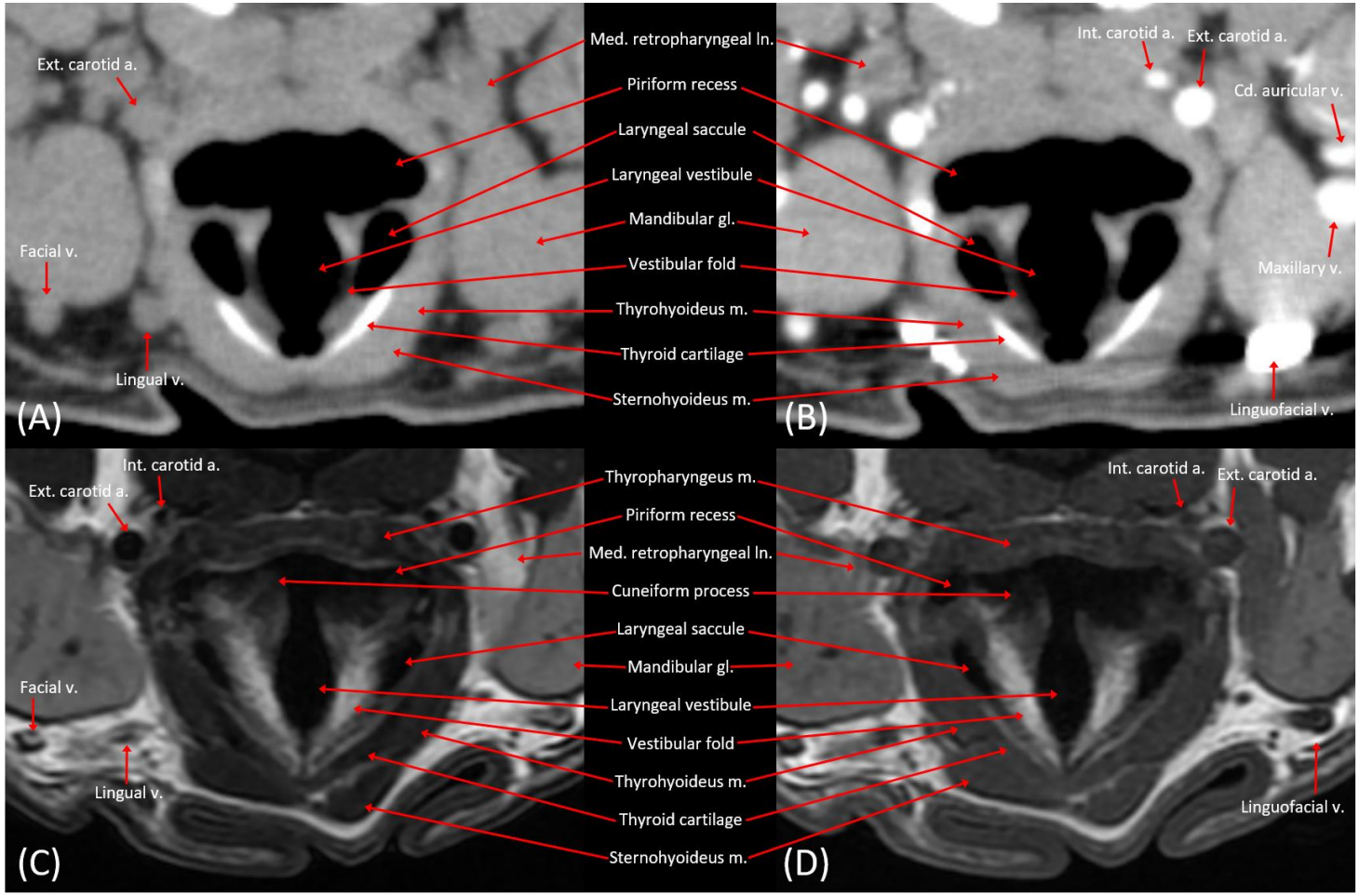

FIGURE 5. Transverse pre- (A) and post-contrast CT (B) images, T2-weighted (C) and T1-weighted MRI (D) at the vestibular fold level (CT window level: 30 HU, window width: 320 HU). The structure that each arrow points to is indicated by its name. The right side of each image is the left side of the animal. Abbreviations: a., artery; Cd. caudal; Ext., external; gl., gland; Int., internal; ln., lymph node; Med., medial; m., muscle; v., vein.

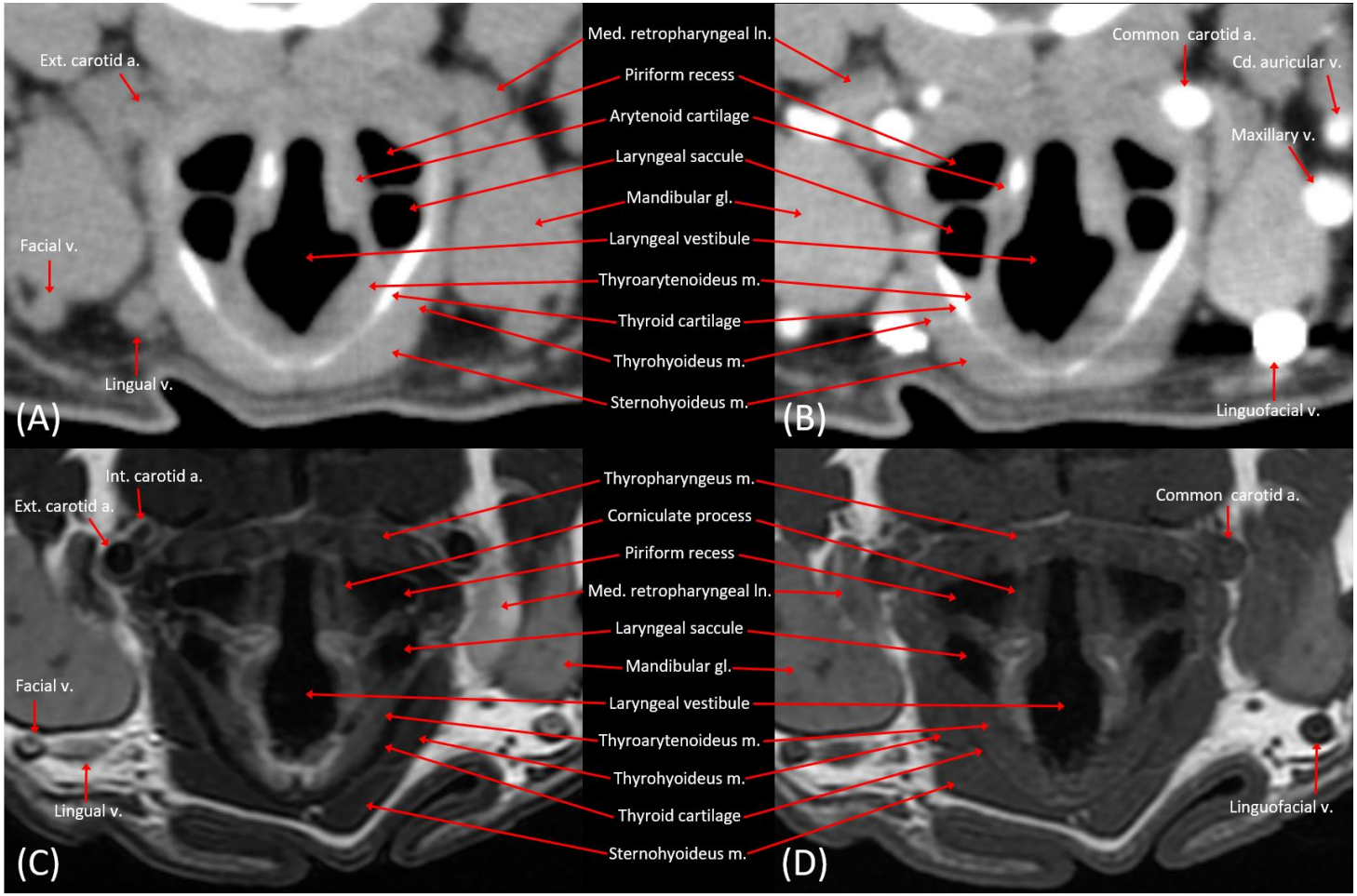

FIGURE 6. Transverse pre- (A) and post-contrast CT (B) images, T2-weighted (C) and T1-weighted MRI (D) at the corniculate process level (CT window level: 30 HU, window width: 320 HU). The structure that each arrow points to is indicated by its name. The right side of each image is the left side of the animal. Abbreviations: a., artery; Cd. caudal; Ext., external; gl., gland; Int., internal; ln., lymph node; Med., medial; m., muscle; v., vein.

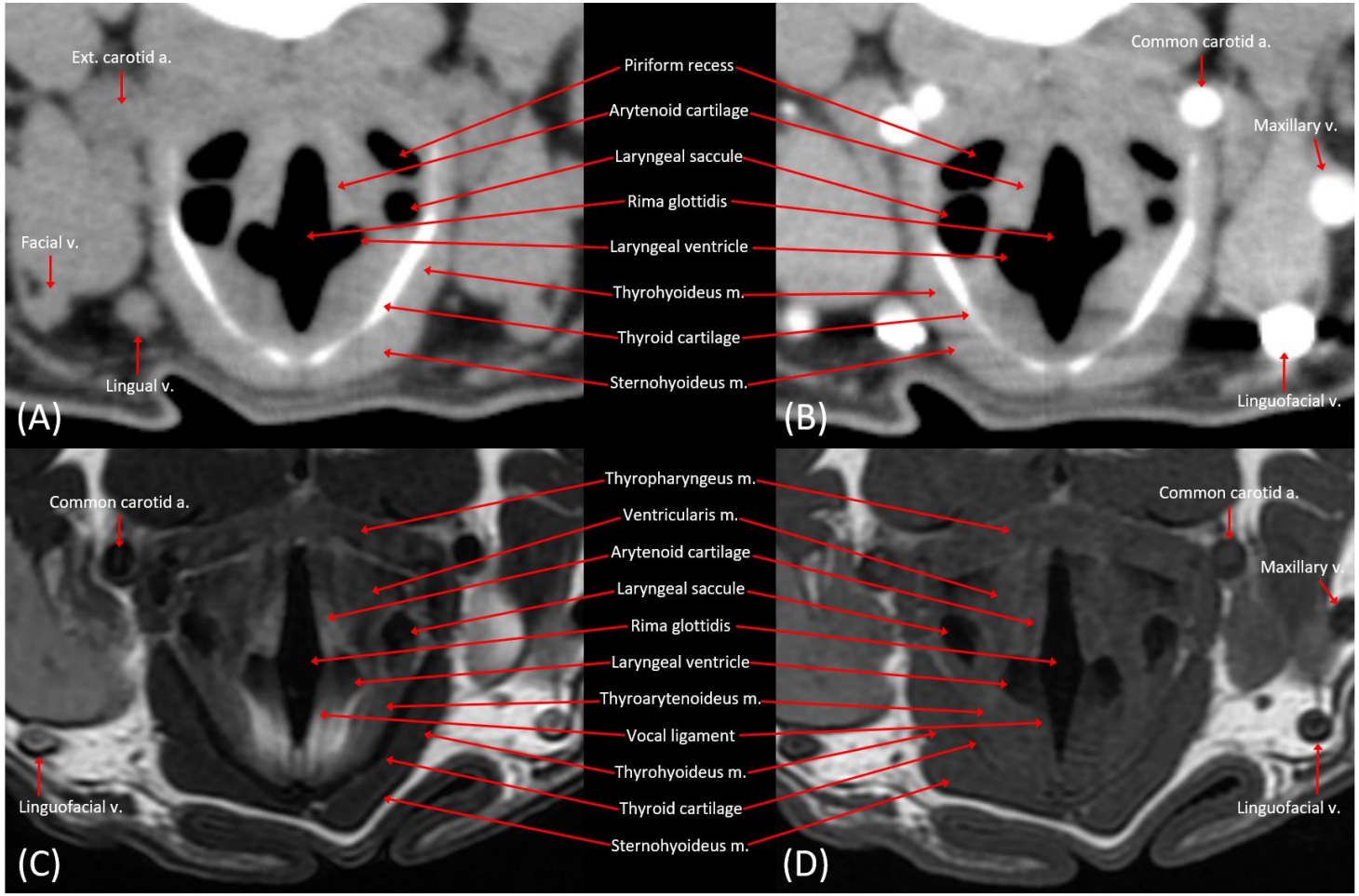

FIGURE 7. Transverse pre- (A) and post-contrast CT (B) images, T2-weighted (C) and T1-weighted MRI (D) at the laryngeal ventricle level (CT window level: 30 HU, window width: 320 HU). The structure that each arrow points to is indicated by its name. The right side of each image is the left side of the animal. Abbreviations: a., artery; Ext., external; m., muscle; v., vein.

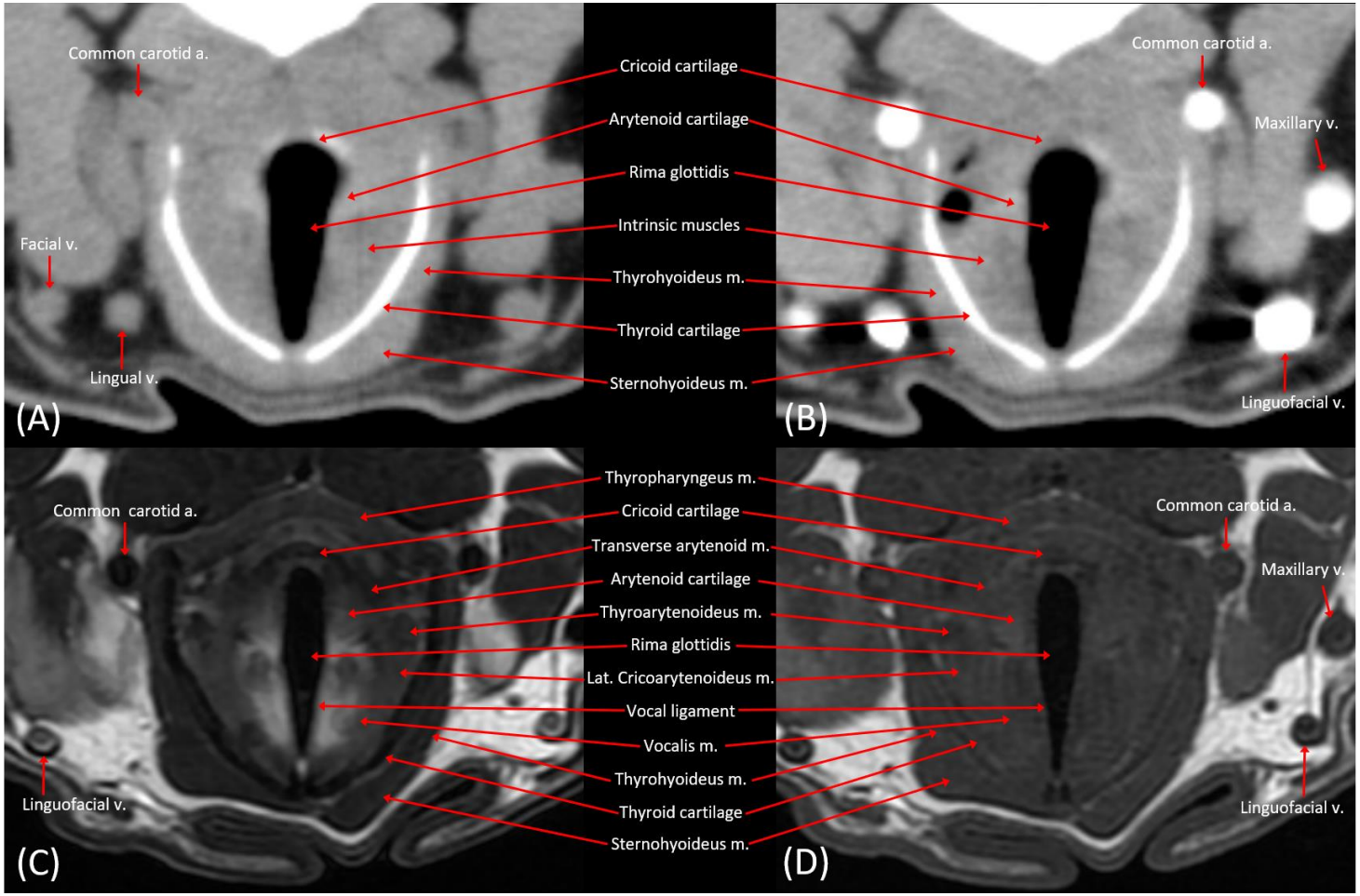

FIGURE 8. Transverse pre- (A) and post-contrast CT (B) images, T2-weighted (C) and T1-weighted MRI (D) at the vocal fold level (CT window level: 30 HU, window width: 320 HU). The structure that each arrow points to is indicated by its name. The right side of each image is the left side of the animal. Abbreviations: a., artery; Lat., lateral; m., muscle; v., vein.

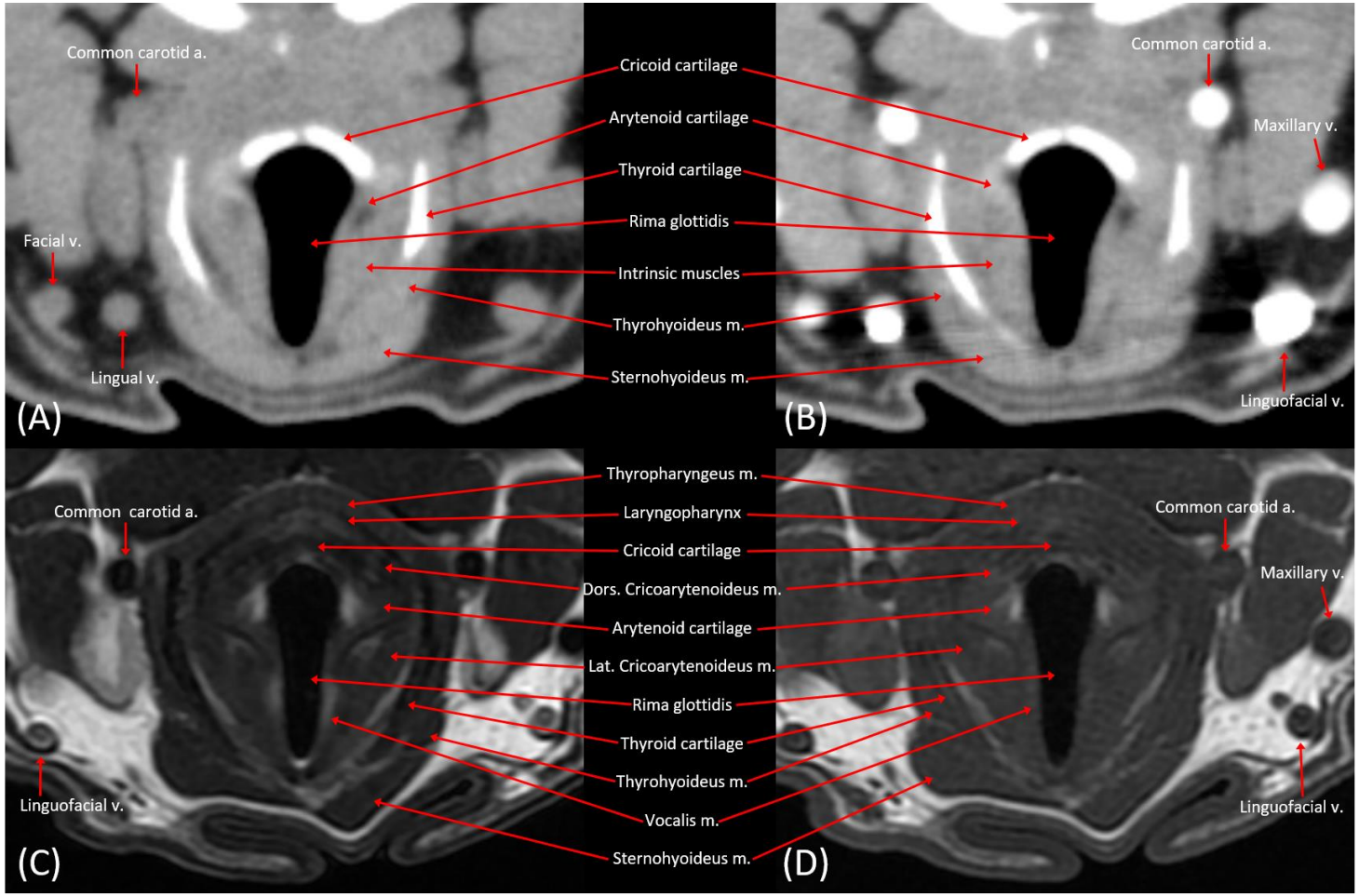

FIGURE 9. Transverse pre- (A) and post-contrast CT (B) images, T2-weighted (C) and T1-weighted MRI (D) at the caudal part of vocal fold level (CT window level: 30 HU, window width: 320 HU). The structure that each arrow points to is indicated by its name. The right side of each image is the left side of the animal. Abbreviations: a., artery; Dors., dorsal; Lat., lateral; m., muscle; v., vein.

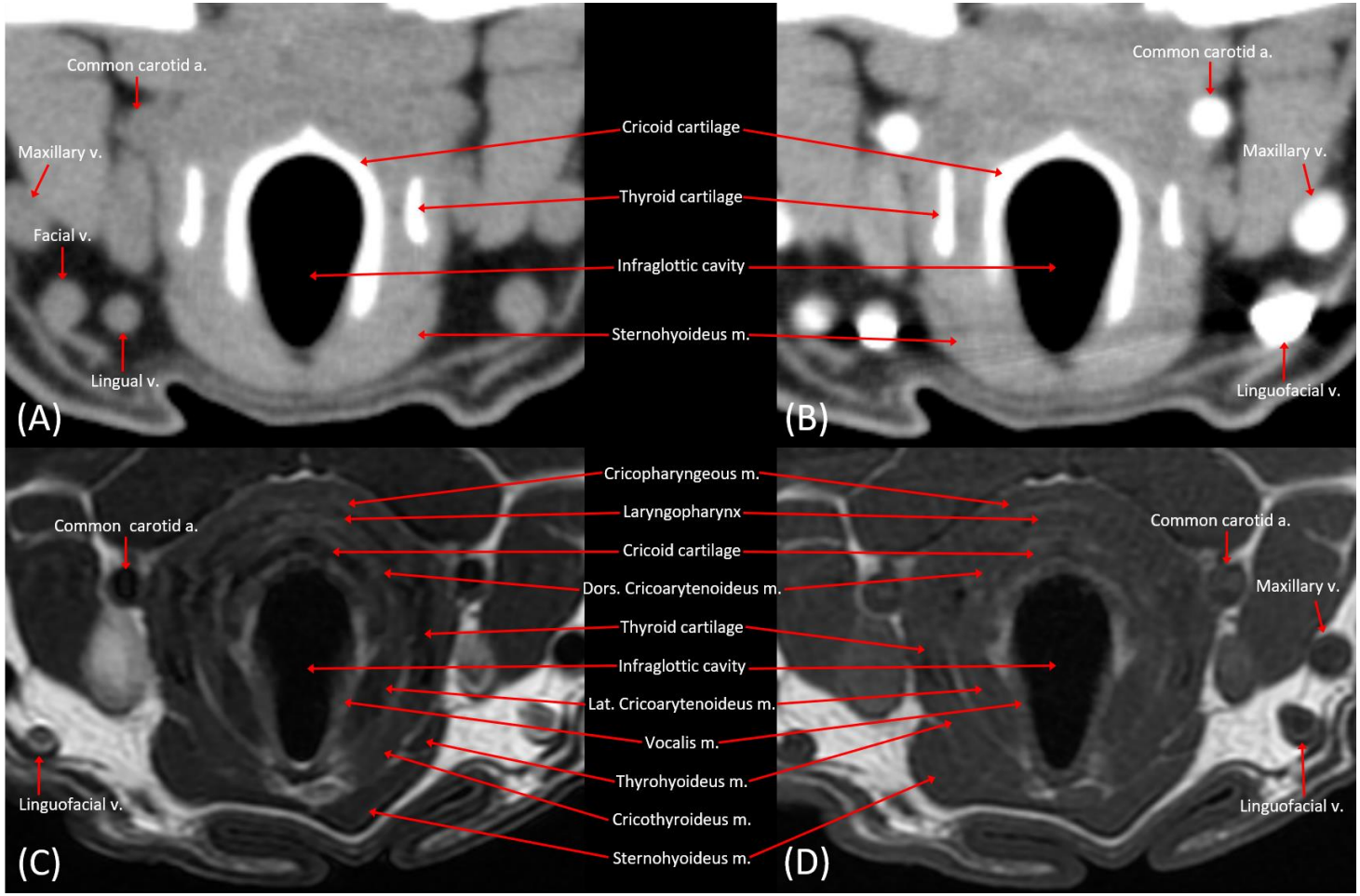

FIGURE 10. Transverse pre- (A) and post-contrast CT (B) images, T2-weighted (C) and T1-weighted MRI (D) at the infraglottic cavity level (CT window level: 30 HU, window width: 320 HU). The structure that each arrow points to is indicated by its name. The right side of each image is the left side of the animal. Abbreviations: a., artery; Dors., dorsal; Lat., lateral; m., muscle; v., vein.

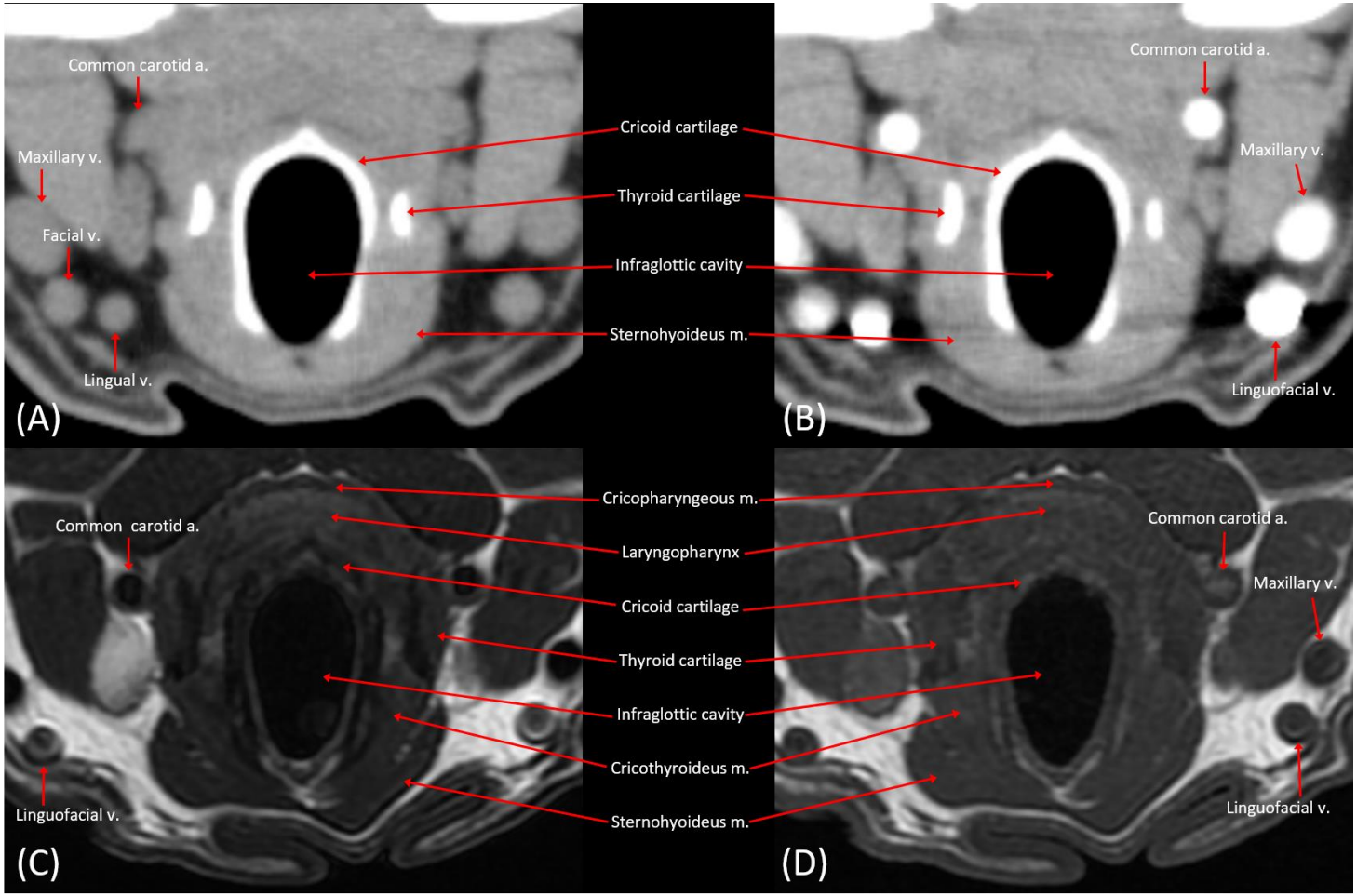

FIGURE 11. Transverse pre- (A) and post-contrast CT (B) images, T2-weighted (C) and T1-weighted MRI (D) at the caudal part of cricoid cartilage level (CT window level: 30 HU, window width: 320 HU). The structure that each arrow points to is indicated by its name. The right side of each image is the left side of the animal. Abbreviations: a., artery; m., muscle; v., vein.

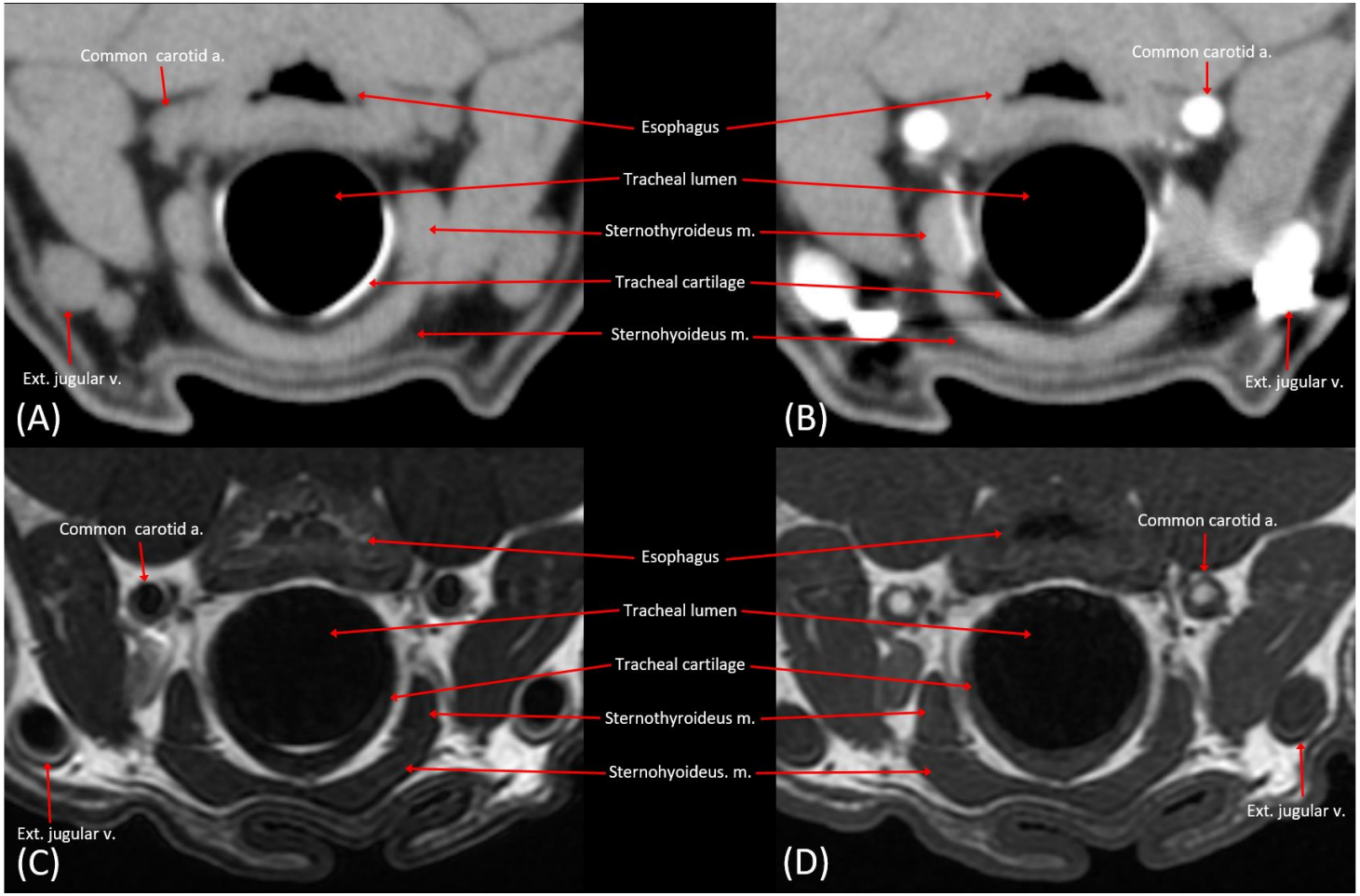

FIGURE 12. Transverse pre- (A) and post-contrast CT (B) images, T2-weighted (C) and T1-weighted MRI (D) at the first tracheal cartilage level (CT window level: 30 HU, window width: 320 HU). The structure that each arrow points to is indicated by its name. The right side of each image is the left side of the animal. Abbreviations: a., artery; Ext., external; m., muscle; v., vein.

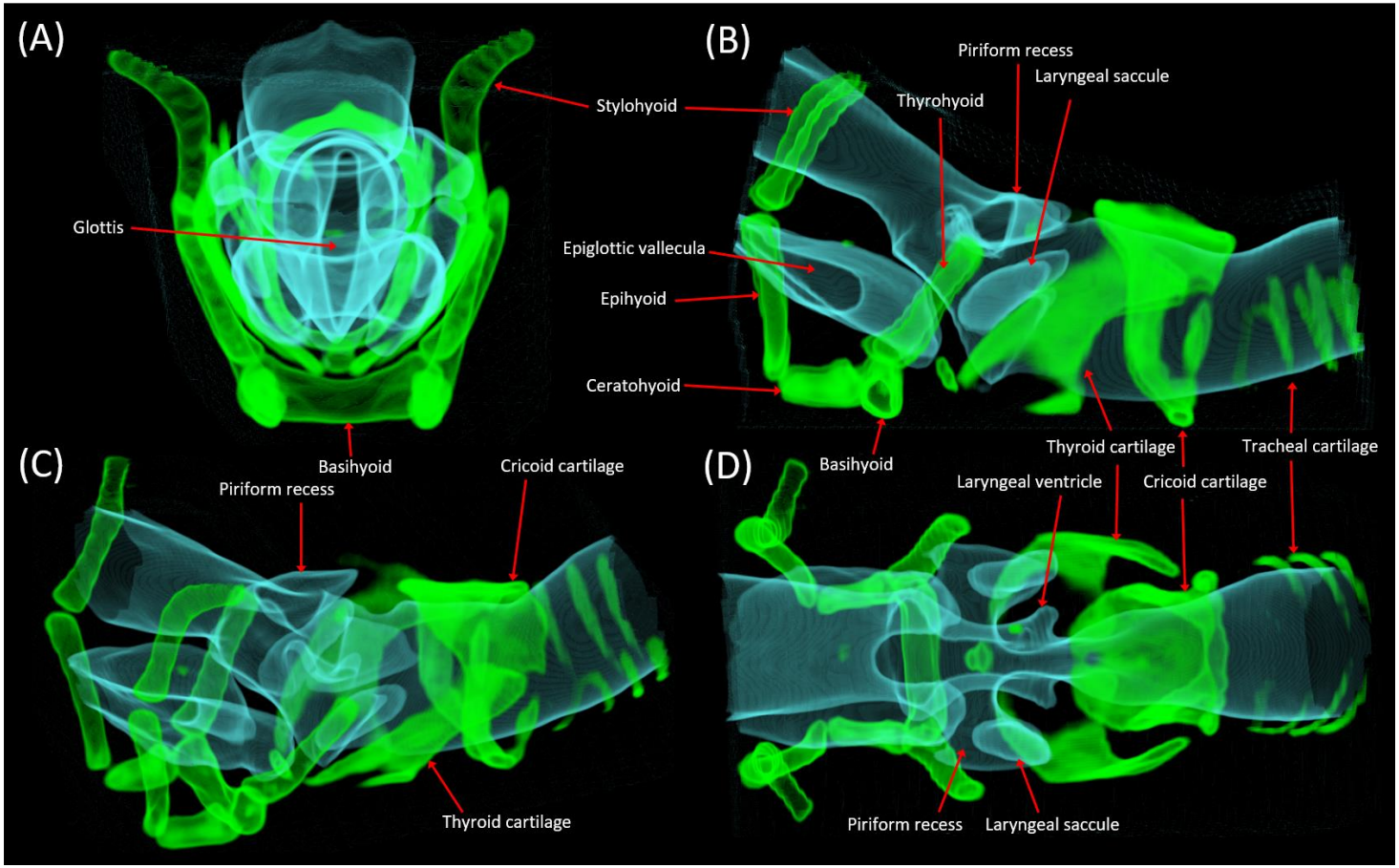

FIGURE 13. 3D volume rendering image of laryngeal region; cranial (A), lateral (B), craniolateral oblique (C), dorsal (D) view. The boundaries of airway and air-filled cavities is expressed in light blue, and structures close to bone density are expressed in green. When the difference in density on CT is obvious, 3D volume rendering is advantageous for comprehending the shape and spatial relationship of complicated structures. The structure that each arrow points to is indicated by its name.

Discussion

In this study, CT and MRI scan of the laryngeal region was performed in clinically normal dogs. Without tracheal intubation, it was possible to acquire MR images capable of detailed evaluation of the laryngeal region only with injection anesthesia. In discrimination of the internal components or conspicuity of soft tissue structures, MRI outperformed CT generally, whereas hyperdense structures such as thyroid cartilage, cricoid cartilage, and the hyoid apparatus were visualized more clearly on CT images.

Air filled cavities and ventricles showed gas attenuation on CT and signal voids on MRI. Blurred appearance of the borders of the piriform recess and laryngeal ventricle on the MR image is thought to be minor artifactual result due to respiratory movement during the scanning period, however, the quality of the images was sufficiently feasible to do the overall evaluation.

At the level between the piriform recess and the laryngeal ventricle based on the transverse section, symmetrical gas attenuation regions were observed and considered as the laryngeal saccule. The laryngeal saccule is the cecal end of the laryngeal ventricle, and it is thought to be observed as an independent sac as the middle part was pressed by the muscle (Done et al., 2009). Although there is no comparable study about this structure in dogs, this structure could be shown due to the dynamic motion according to breathing or posture, considering that there was variation in the size or shape of this structure for each dog.

The epithelium covering from the epiglottis to the vocal fold is non-

stratified squamous epithelium, and the laryngeal epithelium after the vocal fold is gradually changed to a respiratory epithelium (Eurell et al., 2013). Each of the laryngeal cartilages showed slightly different signals. In the case of the epiglottic and arytenoid cartilage, relatively high signal was identified, and these cartilages are elastic cartilage rich in collagen type 2. (Eurell et al., 2013) The laryngeal ligament (vestibular, vocal) also had a high content of type 2 collagen, and the T2W image showed a particularly high signal intensity. On the other hand, the thyroid and cricoid cartilages, which are hyaline cartilage with high collagen type 1 content, showed lower signal intensity (Perez et al., 2010; Vázquez et al., 1998).

In the case of the MRI transverse image of the epiglottis, internal components distinction was less clear than in sagittal, which is thought to be because the cross section of the image is actually an oblique section due to the angle of the epiglottis from the front of the thyroid cartilage to the soft palate. It has been reported that epiglottic cartilage in humans undergoes gradual calcification with age (Kano et al., 2005). The anterior part of the arytenoid cartilage showed a blurred border with artifacts on MRI, and it is considered to be due to movement caused by respiration during scanning, same as the borders of the piriform recess and laryngeal ventricle were blurred.

The laryngeal muscles are composed of intrinsic and extrinsic muscles. Intrinsic muscles move the vocal cord and are responsible for the vocal function of the larynx, while extrinsic muscles cover the outside of the larynx (Tobias et al., 2018). The T1W sequence is mainly used for lesion evaluation with T1W-CE, and is the most commonly used sequence in clinical MRI along with fluid sensitive T2W sequence (Gavin et al., 2009). For the conspicuity of overall laryngeal muscle,

the T2W image showed more distinct contrast than the T1W image, so it was effective to evaluate. The reason why there was no difference between the T1W and T1W-CE images is thought to be because the dogs used in the study were all normal subjects without lesions. It is also considered that the difference between the pre- and post-contrast CT images was not clear for the same reason. If the patient had a lesion in the laryngeal soft tissue region, there would be changes in the post-contrast image.

The hyoid apparatus suspends the tongue root and larynx in the space between the caudal parts of the mandible bodies (Evans et al., 2009). The shape of the hyoid bone was very clearly revealed by the distinct density difference with the surrounding soft tissue structures when the volume rendering technique was applied on the CT image. In patients with suspected hyoid apparatus abnormalities, if the cross-section image and volume rendered image are referred together, it will be helpful to identify the location and morphology of the lesion.

The tongue consists of several muscles with various directions, and in this study, only the root area was included in the scan range. The blood vessels distributed on the tongue were most intuitively confirmed on the post contrast CT images, and when evaluating parenchyma, it was considered that more detailed structures could be evaluated on the MR image than on the CT image.

The soft palate was observed with a homogeneous soft tissue density on the CT image, but the signal difference between the inner muscular and the outer epithelial layer was identifiable on the MR image.

In this research, in normal dogs without respiratory symptoms, sufficient MR images were obtained to evaluate the larynx area through imaging within 1

hour with only intravenous anesthesia, and no respiratory-related side effects were identified during anesthesia and after recovery. However, in the case of patients with upper respiratory problems, there will be practical limitations in maintaining anesthesia for about an hour with only intravenous anesthetics without tracheal intubation. Although tracheal intubation cannot avoid displacement of the internal structure of the larynx, it is expected that the normal anatomical structure identified in this study will still be helpful in locating the lesion. There are additional limitations to this study. All dogs used in this study were male beagles. Therefore, it was not possible to evaluate differences in anatomical structures by breed and sex. In addition, since only dogs in a clinically normal state without abnormalities in the laryngeal region were used in the experiment, imaging was not performed in patients with actual lesions in the corresponding area. Also, maintaining anesthesia for more than 1 hour with intravenous anesthesia alone, as in this study, may be limited in patients with respiratory symptoms or suspected to have abnormalities in laryngeal region.

In conclusion, this study showed that MRI could be applied to assess the normal laryngeal region in dogs only with intravenous anesthesia, without tracheal intubation. Most of the laryngeal structures could be evaluated on both CT and MR images, and structures composed of parenchymal tissue, such as muscles, were better evaluated on MRI especially, whereas hyoid bone or dense laryngeal cartilages were more clearly identified on CT. MR images are considered as sufficiently feasible modality for evaluating the laryngeal region, moreover, it is recommended to prioritize the selection of appropriate modality according to the structure of interest and patient’s condition. The findings of this study could be

utilized to help clinical practitioners choose more appropriate imaging modality for visualizing the laryngeal structures in dogs.

References

Becker, M., Burkhardt, K., Dulguerov, P., & Allal, A. (2008). Imaging of the larynx and hypopharynx. *European Journal of Radiology*, *66*(3), 460–479. https://doi.org/10.1016/j.ejrad.2008.03.027

Carlisle, C. H., Biery, D. N., & Thrall, D. E. (1991). Tracheal and Laryngeal Tumors in the Dog and Cat: Literature Review and 13 Additional Patients. *Veterinary Radiology*, *32*(5), 229–235. https://doi.org/10.1111/j.1740-8261.1991.tb00112.x

Done, S. H., Goody, P. C., Evans, S. A., & Stickland, N. C. (2009). *Color Atlas of Veterinary Anatomy* (3rd ed.). Mosby.

Dunbar, M. D., Ginn, P., Winter, M., Miller, K. B., & Craft, W. (2012). Laryngeal rhabdomyoma in a dog. *Veterinary Clinical Pathology*, *41*(4), 590–593. https://doi.org/10.1111/j.1939-165x.2012.00484.x

Elders, B. B. L. J., Hermelijn, S. M., Tiddens, H. A. W. M., Pullens, B., Wielopolski, P. A., & Ciet, P. (2019). Magnetic resonance imaging of the larynx in the pediatric population: A systematic review. *Pediatric Pulmonology*, *54*(4), 478–486. https://doi.org/10.1002/ppul.24250

Eurell, J. A., & Frappier, B. L. (2013). *Dellmann's Textbook of Veterinary Histology* (6th ed.). Wiley-Blackwell.

Evans, H. E. & Lahunta, A. L. (2009). *Guide to the Dissection of the Dog* (7th ed.). Saunders.

Evans, H. E. & Lahunta A. L. (2012). *Miller's anatomy of the Dog* (4th ed.). Elsevier.

Gavin, P. R., Bagley, R. S. (2009). *Practical small animal MRI*. Wiley-Blackwell. https://doi.org/10.1002/9780813810324

Tobias, K. M. & Johnston, S.A. (2018). *Veterinary surgery: Small animal*. Elsevier.

Kano, M., Shimizu, Y., Okayama, K., Igari, T., Kikuchi, M. (2005). A morphometric study of age-related changes in adult human epiglottis using quantitative digital analysis of cartilage calcification. *Cells Tissues Organs, 180(2),* 126–137. DOI: 10.1159/000086753

MacPhail, C. M. (2020). Laryngeal disease in dogs and cats: an update. *Veterinary Clinics of North America: Small Animal Practice*, 50(2), 295-310. https://doi.org/10.1016/j.cvsm.2019.11.001

Perez, B., Gomez, M., Mieres, M., Galecio, J. S., Yefi, C., & Aburto, P. (2010). Computed tomographic anatomy of the larynx in mesaticephalic dogs. *Archivos de Medicina Veterinaria*, *42*(1), 91–99. https://doi.org/10.4067/S0301-732X2010000100013

Perinetti, G. (2018). StaTips Part IV: Selection, interpretation and reporting of the intraclass correlation coefficient. *South European Journal of Orthodontics and Dentofacial Research*, *5*(1), 3–5. https://doi.org/10.5937/sejodr5-17434

Stadler, K., Hartman, S., Matheson, J., & O'Brien, R. (2011). Computed tomographic imaging of dogs with primary laryngeal or tracheal airway obstruction. *Veterinary Radiology and Ultrasound*, *52*(4), 377–384. https://doi.org/10.1111/j.1740-8261.2011.01816.x

Teixeira, P. P. M., Souza, E. S., Jark, P. C., Coutinho, L. N., da Silva, A. S. L., Guiduce, M. V. S., . . . Nardi, A. B. (2014). Endoscopic approach for a laryngeal neoplasm in a dog. *Ciencia Rural*, 45(1), 131–135. https://doi.org/10.1590/0103-8478cr20131084

Vázquez, J. M., Arencibia, A., Gil, F., Ramírez, J. A., González, N., Sosa, C. D., & Jaber, J. R. (1998). Magnetic resonance imaging of the normal canine larynx. *Anatomia, Histologia, Embryologia*, *27*(4), 263–270. https://doi.org/10.1111/j.1439-0264.1998.tb00191.x

Wu, J. H., Zhao, J., Li, Z. H., Yang, W. Q., Liu, Q. H., Yang, Z. Y., . . .Lei, W. B. (2016). Comparison of CT and MRI in diagnosis of laryngeal carcinoma with anterior vocal commissure involvement. *Scientific Reports*, 6, 30353. https://doi.org/10.1038/srep30353

국문초록

개에서 정맥마취 하 자기공명영상을 통한 정상 후두 부위의 해부학적 평가

서울대학교 대학원
수의학과 임상수의학 전공
백 록 담

호흡 마취를 위한 기관 삽관은 후두를 이루는 구조물들의 변위를 일으키고, 진단영상에서 병변을 있는 그대로 평가하는 것을 어렵게 한다. 이러한 이유로, 장시간의 검사 시 마취가 필수적인 수의학에서 후두 부위에 대한 MRI 연구는 드물게 이루어졌다. 본 연구의 목적은 기관 삽관 없이 정맥마취만으로 후두 부위에 대한 MRI 촬영의 임상적 활용 가능성을 평가하는 것이었다. 실험에는 호흡기 임상증상이 없는 5마리의 수컷 비글 실험견을 사용하였고, 주사마취 후 조영 전, 후 CT촬영에 이어 MRI 촬영 순서로 진행하였다. 영상 촬영 장비는 1.5-Tesla MRI와 64-slice CT scanner를 이용하였다. MRI의 임상적 활용의 타당성을 평가하기 위해 세 명의 관찰자가 CT와 MRI 영상 상 후두를 이루는 구조물들의 식별 및 구조물들의 층 구별 정도를 점수화하였고, 통계 처리 후 결과를 비교하

였다. 관찰자 간 일치도 분석을 위한 급내상관계수는 매우 높은 일치도를 보였다. 윤상연골, 갑상연골, 설골의 식별에는 MRI의 활용도가 뚜렷한 밀도차를 반영하는 CT 영상보다 다소 낮을 것으로 고려되었다. 반면, 성대인대, 후두 근육의 식별, 그리고 연골들의 층 구별 등 연조직의 세세한 평가에는 MRI의 활용도가 높을 것으로 고려되었다. 호흡 시 움직임에 의해 발생하는 것으로 생각되는 허상은 피열연골의 경계 일부를 약간 흐리는 정도로 확인되었으며 영상 평가에 큰 지장을 주지는 않았다. MRI는 후두 부위 평가에 적용 가능한 영상기법으로 고려되며, 나아가 본 연구 결과가 실제 환자의 병변이 의심되는 세부 부위에 따른 진단기법 선택 시 도움이 될 것으로 기대된다.

주요어: 개, 후두, 컴퓨터단층촬영, 자기공명영상

학 번: 2021-26846